ISTFA™ 2019: Conference Proceedings from the 45th
International Symposium for Testing and Failure Analysis
November 10–November 14, 2019, Portland, Oregon, USA
DOI: 10.31399/asm.cp.istfa2019p0043

Solder bump joint failure investigation: From sample preparation to advanced structural characterizations and strain measurements

Pawel Nowakowski, Mary Ray, and Paul Fischione
E.A. Fischione Instruments, Inc., Export, PA, USA

Abstract

This paper describes the detailed sample preparation of a solder joint at the level between a semiconductor package and board. Different sample preparation techniques are described and compared. Preparing and targeting a large sample area containing multiple solder bumps is discussed. The sample preparation methods will then be confirmed by advanced structural characterization and strain measurement. The presence of strain is associated with the development of cracks and delamination at the solder joint interface.

Introduction

The packaging technologies of microelectronic flip chips involve solder joints that connect the chip and board. To guarantee reliability of microelectronic devices, the prediction of solder joint failures and their early state detection is critical. Both leaded and lead-free solder bumps are used as joints. Because of constantly decreasing solder bump dimensions and pitch, defect detection and investigation is becoming more challenging. An accurate, reliable, and easy-to-use investigation technique is critical for solder joint defect inspection in high density microelectronic packaging [1-5].

One of the most critical failures of this joint is the loss of connectivity between copper pads and solder bumps, which appears in the form of cracks or delamination. These defects result from joint microstructural evolution induced by constant or cyclic loading conditions during device service. The strain accumulated at the interface between solder bump and copper pad can lead to joint failure. Therefore, an understanding of the joint structure evolution and knowledge about the strain state at the joint interface can provide insight into the failure mechanism and prevent it in the future.

A solder joint is typically made of a Sn-based alloy (solder material), an intermetallic compound at the joint interface, and copper pad. Tin is a very soft and ductile material that can be very easily deformed, i.e., any exterior intervention to the joint can lead to structural change. For that reason, preparation of solder bump samples is typically a delicate and potentially complex process. Any mechanical action, such as cutting, grinding, and polishing, can provoke structural changes and introduce strain at the joint interface that leads to cracks and delamination. A sample preparation technique that preserves the native state of the joint structure without introducing any artifacts is necessary to fully understand the failure mechanism. In this paper, we first look for an appropriate sample preparation technique that allows the preservation of the solder joint's native state. Second, we concentrate on structural characterization and strain measurement at the joint interface.

To illustrate our unique solder bump characterization approach, we consider two samples:

- Device #1: A chip package with solder bumps ready to be installed on the board (Figure 1).
- Device #2: A chip package already installed on the board, which was extracted from a commercially available "smart" phone (Figure 2).

Two sample preparation techniques are considered for comparison purposes: Mechanical polishing (MP) and argon broad ion beam milling (BIB).

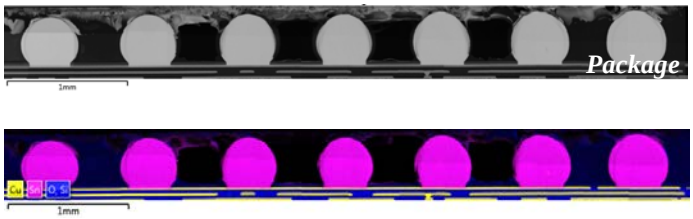

Figure 1. Cross-section image of a chip package with solder bumps ready to be put on a board. The cross-section sample was created by argon BIB milling. Back-scattered electron (BSE) contrast image of seven bumps on the package (a) and EDS overlay maps of Cu, Sn, O, and Si (b).

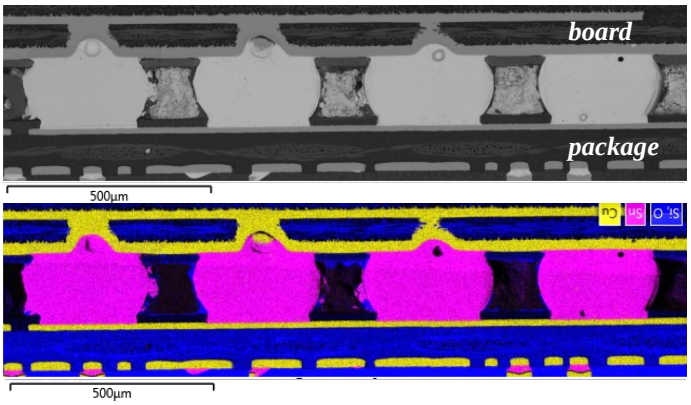

Figure 2. Cross-section image of a chip package connected to a board. The cross-section sample was created by argon BIB milling. BSE contrast image of four bumps located between the package and board (a) and EDS overlay *maps of Cu, Sn, O, and Si (b).*

Sample preparation

Two sample preparation techniques were used: MP and argon BIB milling. The MP technique consists of polishing using abrasives. The sample was polished using #800- and #1200-grade SiC papers (for 3 minutes or less per paper grade). The sample was then polished using 3, 1, and 0.5 µm diamond particles in oil suspension; the polishing times increased from 5 to 15 minutes as the particle size decreased. The last step of the MP process was colloidal silica (0.05 µm particles) polishing for 2 hours. The total MP time, including cleaning could take up to 4 hours. In contrast, the BIB technique required only 20 minutes to 1 hour of processing depending on sample surface finished prior to the process.

The BIB technique consists of material removal (polishing) by action of argon ions accelerated to a user-specified energy between 0.1 eV to 10 keV. The ions form a beam with a user-specified beam current value. The process is commonly known as ion milling. In this manuscript, all samples, after MP process, and prior to ion milling, were repolished using 1 µm and 0.5 µm diamond pastes. The following ion milling conditions were used:

- **Beam energy:** 6 keV for 20 minutes, followed by 4 keV for 40 minutes.
- **Beam angle:** 3° (grazing angle).
- **Beam angle:** 3° (grazing angle).
- **Stage cooling:** Because of tin solder bump thermal sensitivity, liquid nitrogen was used to cool the ion mill's sample stage to -150 °C during milling.

MP (Figure 3a) and BIB milling (Figure 3b) scanning electron microscopy (SEM) observations show that results of each technique appear to be similar. However, sample surface cleaning after MP (colloidal silica suspension) was very difficult. The SiO_2 particles stuck to the sample surface and were very difficult to remove. Attempts to remove the particles led to the introduction of scratches on the soft tin and copper that damaged the joint interface. In addition, the use of water for cleaning provoked corrosion of different package components and made the polishing and cleaning process very complex.

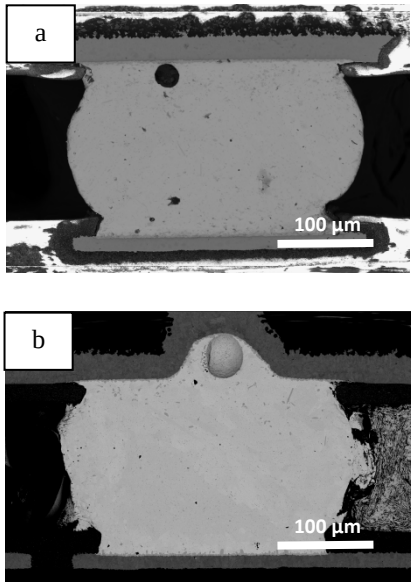

Figure 3. BSE contrast image of solder joints after mechanical polishing (a) and after argon BIB milling (b).

Sample preparation technique evaluation

Electron backscatter diffraction (EBSD) was used to perform structural characterization; high resolution EBSD (HR-EBSD) was used to perform strain measurements. Figure 4 shows EBSD analyses of the solder bumps prepared by MP and argon BIB milling. In the MP sample, the area close to the joint interface (Figure 4a, yellow square) cannot be analyzed by the EBSD technique. The copper pad caused a shadowing effect due to the difference in material removal during mechanical polishing. In addition, corrosion product from package components contaminated (Figure 4a, green squares) the area of interest; these areas also cannot be analyzed by the EBSD technique. In contrast, the sample prepared by argon BIB milling (Figure 4b) produced excellent quality EBSD patterns – the entire tin bump and the copper pad (including the joint interface) were visualized. From such high-quality sample preparation, accurate microstructural analyses and strain localization and measurements were possible. Figure 4 shows the grain structure, size, and crystallographic orientation of the tin bump and the copper pads.

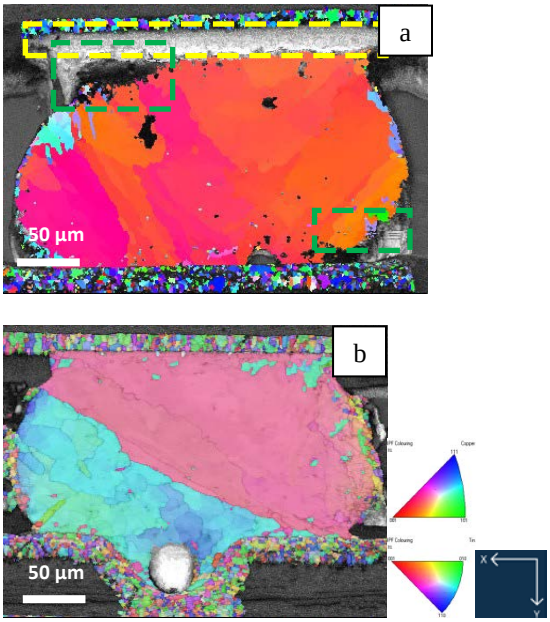

Figure 4. EBSD inverse pole figure (IPF) orientation maps overlaid on band contrast maps collected from solder joints after: (a) mechanical polishing (yellow square indicates that the solder bump is shadowed by the copper pad; green squares indicate areas where corrosion product from packaging components redeposited onto the area of interest); and (b) after argon BIB milling.

Strain measurements results and discussion

The strains were first localized using local misorientation measurement from the EBSD data (Figure 5). Next, the strains were measured by HR-EBSD technique [6-9] (Figures 6 and 7). Only the argon BIB milled samples were of high enough quality to undergo strain evaluation investigation.

Figure 5 clearly shows a difference in the strain present in the sample of the device package not connected to a board (Figure 5a) and a device package connected to a board (Figure 5b). Strain evaluated from local misorientation measurements clearly show an absence of deformation in device 1 (Figure 5a). In contrast, device #2 shows strain accumulated at the interface of the solder bump and copper pad (Figure 5b, red square) and at the area between the solder bump void and copper pad (Figure 5b, black square). In these two areas, there is a high probability for failures (cracks or delamination) to occur.

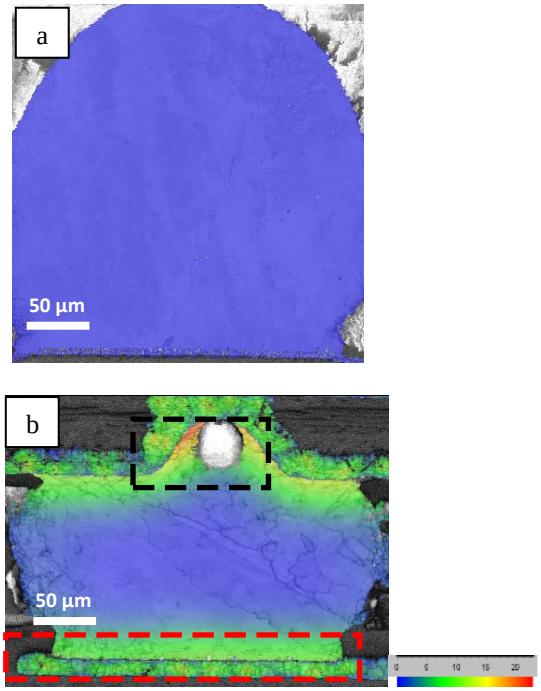

*Figure 5. Strain contouring EBSD map of a solder joint after argon BIB milling: a) **device #1** not connected to a board; b) **device #2** connected to a board. Strain accumulated at the interface of the solder bump and copper pad (b, red square) and at the area between the solder bump void and copper pad (b, black square).*

HR-EBSD measurements were carried out at this early state of deformation, which preceded the appearance of cracks or delamination. Figure 6 shows the average total effective strain measured by HR-EBSD analyses. Total average effective strain for device #1 was of 10^{-3} order of magnitude (Figure 6a), while for device #2, the effective strain was much higher: 10^{-2} order of magnitude (Figure 6b). The accumulation of strain is clearly observed in the solder bump area close to the copper pad (Figure 6b).

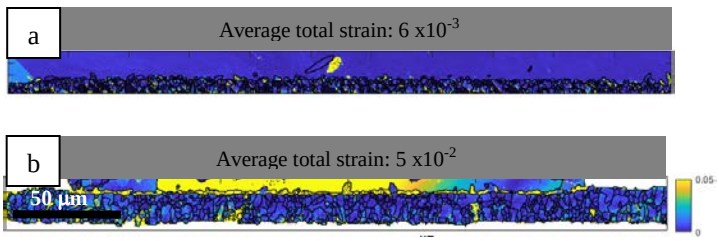

Figure 6. Average total effective strain from HR-EBSD measurements for device #1 (a) and device #2 (b).

To better understand how strain accumulated and the deformation process, we investigated strain fields obtained for principal strain components ε_{xx}, ε_{yy}, and ε_{zz} (Figures 7 and 8). The results show average elastic strain is lower by up to two orders of magnitude between device #1 and device #2. For device #1 (Figure 7), strain was uniformly distributed around the zero value of the scale ($x10^{-5}$ magnitude order). In contrast, device #2 (Figure 8) strain was primarily localized at the solder bump/copper pad interface. High positive strain present in a normal (ε_{zz}) direction, a compressed (negative) strain in the horizontal (ε_{xx}) direction, and mixed strain in the transverse (ε_{yy}) direction were observed (Figure 8). This indicates that complex loading conditions acted on the solder bump between the package substrate on the one side and the board on the other side.

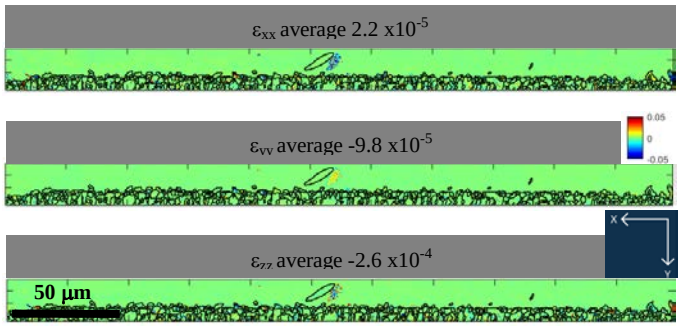

Figure 7. Device #1 HR-EBSD strain field obtained for principal strain components: ε_{xx}, ε_{yy}, and ε_{zz}.

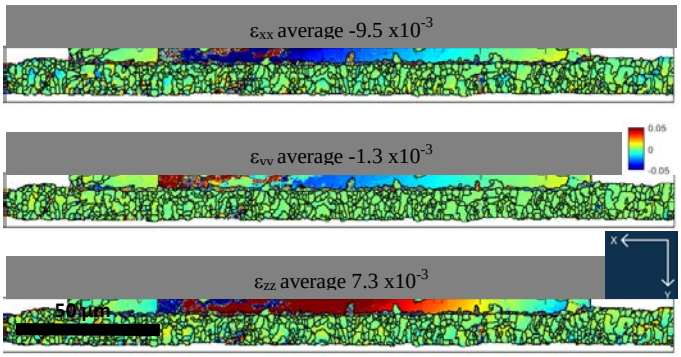

Figure 8. Device #2 HR-EBSD strain field obtained for principal strain components: ε_{xx}, ε_{yy}, and ε_{zz}.

Conclusion

A comparison of sample preparation methods for solder bump failure investigation was presented. The argon BIB milling was found superior to MP because argon BIB milling because it did not

introduce additional mechanical stress or defects to the sample.
In addition, argon BIB milling allowed accurate structure and microstructure investigation of the solder junction, which included advanced strain quantification.

The presence of strain is associated with the development of cracks and delamination at the solder joint interface; understanding the strain characteristics is the first step toward understanding the failure mechanism and, ultimately, how to prevent these types of failures in the future.

References

[1] Liu, A. et al. (2011). Characterization of fine-pitch solder bump joint and package warpage for low K high-pin-count flip-chip BGA through shadow moiré and micro moiré techniques. In *2011 IEEE 61st Electronic Components and Technology Conference (ECTC)* (pp. 431-440). Lake Buena Vista, FL: IEEE.

[2] Fan, M. et al. (2016). Defect inspection of solder bumps using the scanning acoustic microscopy and fuzzy SVM algorithm. *Microelectronics Reliability*, *65*, 192-197. doi:10.1016/j.microrel.2016.08.01

[3] Kang, S. K., Gruber, P., and Shih, D. (2008). An overview of Pb-free, flip-chip wafer-bumping technologies. *JOM*, *60*(6), 66-70.

[4] Mercado, L. et al. (2003). Analysis of flip-chip packaging challenges on copper/low-k interconnects. *IEEE Transactions on Device and Materials Reliability*, *3*(4), 111-118.

[5] Mallik, D. et al. (2005). Advanced package technologies for high-performance systems. *Intel Technology Journal*, *09*(04), 259-271.

[6] K.Z. Troost, et al., (1993). Microscale elastic strain determination by backscatter Kikuchi diffraction in the scanning electron microscope. *Applied Physics Letters 62 (10)*, 1110-1112.

[7] A. Wilkinson, et al., (1996). Measurement of elastic strains and small lattice rotations using electron back scatter diffraction. *Ultramicroscopy 62*, 237-247.

[8] A. Wilkinson, et al., (2006). High-resolution elastic strain measurement from electron backscatter diffraction patterns: new levels of sensitivity. Ultramicroscopy 106 307-313.

[9] T.B. Britton, et al., (2011). Measurement of residual elastic strain and lattice rotations with high resolution electron backscatter diffraction. Ultramicroscopy 111(8) 1395-1404.